

NOISE TEMPERATURE FOR Nb DHEB MIXER RECEIVER FOR FAR-INFRARED SPECTROSCOPY

E. Gerecht, C. D. Reintsema, and E. N. Grossman

National Institute of Standards and Technology
Boulder, CO 80305

A. L. Betz and R. T. Boreiko

Center for Astrophysics & Space Astronomy, University of Colorado
Boulder, CO 80309

ABSTRACT - We are reporting a noise temperature measured on a diffusion-cooled hot electron bolometric (DHEB) mixer designed for a heterodyne focal plane array to study lines with frequencies of 2 THz and above. Our fabrication process utilizes selective ion milling techniques to produce Nb diffusion-cooled hot-electron bolometric mixers from a bilayer thin film of Au/Nb deposited on a silicon substrate. A microbridge of Nb 12 nm thick forms the HEB device. The devices are fabricated at the leads of a broad-band spiral antenna with a frequency response of up to 16 THz. A far-infrared (FIR) laser was used as the local-oscillator (LO) source at 2.52 THz (119 μm). A double-sideband (DSB) receiver noise temperature of 2500 K was measured. The IF frequency determined by the cold amplifier was centered at 1 GHz. This noise temperature result is not corrected for losses and mismatches and was performed at a bath temperature of 2 K. The device has a critical temperature (T_c) of 6 K and a 0.5 K transition width.

** Publication of the National Institute of Standards and Technology, not subject to copyright.*

I. INTRODUCTION

Observations of spectral line have played a major role in expanding our understanding of the interstellar medium and planetary atmospheres. Heterodyne spectroscopy is capable of providing the required sensitivity and spectral resolution over the entire far-infrared spectral region. However, future observations will require more sophisticated receivers with quantum noise limited sensitivity and multiple mixer elements in the focal plane. Although small arrays have been demonstrated in millimeter wave receivers, none have been developed for

far-infrared receivers for the 1-5 THz band. An array as simple as 4 elements would provide a significant enhancement in line mapping capabilities, especially on airborne telescope such as SOFIA.

Until recently GaAs Schottky barrier diodes (SBD) were used almost exclusively for heterodyne receivers in the THz region. Below 1 THz, SIS (Superconductor/Insulator/Superconductor) mixer receivers have excellent noise temperature (only a few times the quantum noise limit). The noise performance is limited to frequencies below or about equal to the superconducting bandgap frequency. Hot electron bolometric (HEB) mixers, which use nonlinear heating effects in superconductors near their transition temperature [1], have become an excellent alternative for applications requiring low noise temperatures at frequencies from 1 THz to 5 THz. There are two types of superconducting HEB devices, the diffusion-cooled (DHEB) version [2][3] and the phonon-cooled (PHEB) version [4]. The two versions differ mainly by the cooling mechanism of the hot electrons. The devices under development here are DHEBs with a projected local oscillator (LO) power requirement of less than 100 nW and bath temperature of less than 2 K. The present state of the art of different THz receivers is compared in FIG. 1.

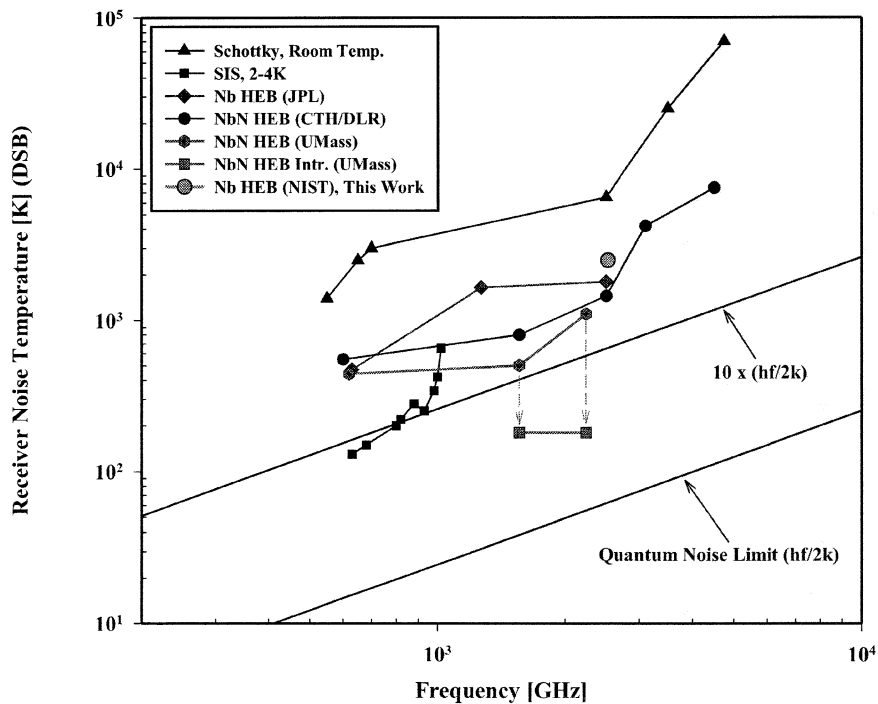


FIG. 1. Noise temperatures vs. frequency for receivers in the terahertz regime [5]-[8].

II. DEVICE DESIGN AND FABRICATION

A quasi-optical coupling design was chosen [9] for our work. The focal plane array is of the “fly-eye” configuration, with individual substrate lens for each of the 4 pixels. (Obviously, this configuration is suitable only for arrays of relatively small format.) The incoming energy couples to the device through an elliptical lens 4 mm in diameter, made from high-purity silicon and no AR coating, and a spiral antenna with a maximum frequency response of 16 THz [10]. The spiral wrap angle is 20 degrees, with a nominal separation of the feedpoints of 1.2 μm . The spiral design is self-complementary, implying an antenna impedance of 75 Ω . The array includes two antennas with 2 1/4 turns and two with 2 3/4 turns, which imply lower frequency limits of 520 GHz and 160 GHz, respectively. These approximate frequency limits are derived from the criterion that the antenna radius be equal to 1/4 of an effective wavelength. The radius of the inner edge of the antenna is used for the upper frequency limit and the outer edge for the lower frequency limit, with an additional quarter-turn left for engineering margin. The IF signal is coupled out of the HEB thru a 50 Ω coplanar waveguide (CPW), the center conductor of which contacts the center conductor of a microminiature K-type connector. The CPW groundplane is common to all four array elements, and directly contacts the body of the mixer block through an indium foil “gasket”. The 4 element array configured with lenses and spiral antennas is shown in FIG. 2.

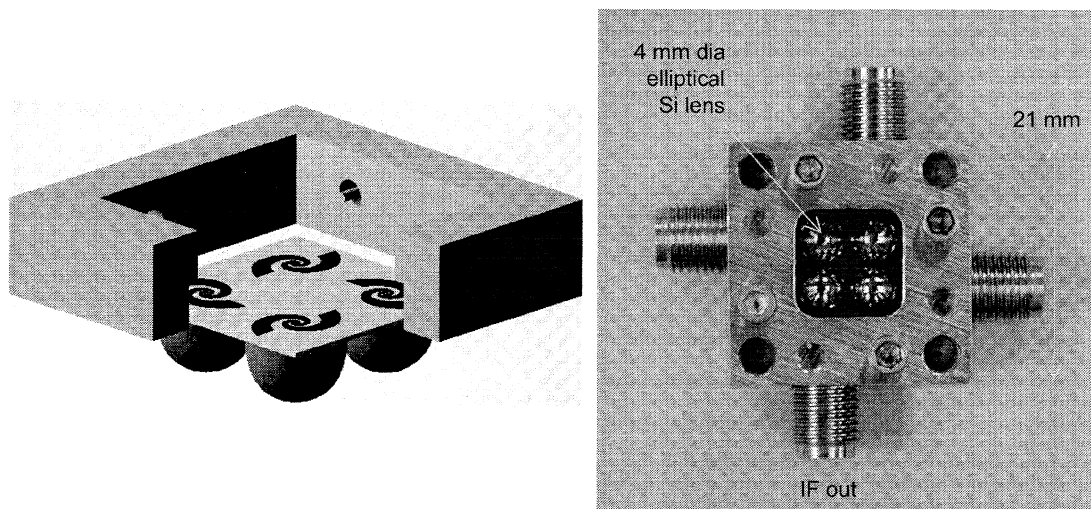


FIG. 2. Array configuration; on the left, a conceptual rendering showing the chip with four elements and substrate lenses, on the right, a photograph of the assembly.

A typical device fabrication begins with the deposition of a uniform bilayer metallic film across a silicon wafer that has been thermally oxidized to a thickness of 300 nm. The bilayer is composed of a 12 nm niobium base layer capped by 20 nm of gold (see FIG. 3). The films are deposited in-situ using DC magnetron sputtering. The HEBs are ultimately formed in the base Nb layer as the last step of the process. The gold cap layer is intended to protect the Nb during initial fabrication steps as well as to mitigate contact-resistance problems between the device and overlying metallic layers. Following the bilayer deposition, a gold layer 100 nm thick is deposited through a photoresist liftoff mask patterned by use of conventional UV lithography. This mask defines the log spiral antennas, ground plane, and the coplanar waveguide feed structure to the four array elements. The gold is deposited using thermal evaporation following a 1 minute Ar RF plasma cleaning step to treat the contact regions.

Since optical lithography is used for the antenna patterning, the lead separation at the feed of the antenna remains much too large ($\sim 2 \mu\text{m}$) for the dimensions of useful HEB devices. Therefore, a second contact metallization step, using E-beam lithography (EBL), to define the length scale of the devices was performed. Again gold lift-off is used, but through an EBL-patterned PMMA mask in this case. Finally, 50 nm of Au are deposited with an electrode separation of between 80 and 100 nm at the antenna feed. The deposition process is the same as for the antenna layer.

The last few steps of the process have produced a structure, depicted in FIG.3(c), which includes a complete antenna structure over a blanket Nb/Au bilayer. The 20 nm Au bilayer cap is then removed in an Ar ion mill using the thick gold as a sacrificial mask. There is no additional patterning associated with this step. The 30 nm of the antenna and contact Au are sacrificed to clear the bilayer surface gold from the underlying Nb in the open field areas. The ion mill process has reasonable selectivity to Au as compared to Nb ($>5:1$).

At this point the device has a Nb layer underlying the entire structure as evident in FIG. 3(e). This Nb must be cleared everywhere except for the final device region. This is accomplished in a two-step reactive-ion etch (RIE) process. The first step uses optical lithography to pattern a mask that protects a $6 \mu\text{m} \times 6 \mu\text{m}$ square region centered over each device. The chip is then subjected to a SF_6 RIE process to clear the Nb in the exposed field regions (see FIG.3(f)). The chip is then patterned one last time using EBL to leave a narrow strip of PMMA bridging the gap between the Au contacts and protecting the final device area. The width of this strip, nominally 10 to 20 nm, defines the final width of the HEB. There is a $10 \mu\text{m} \times 10 \mu\text{m}$ window around this strip that fully encompasses the $6 \mu\text{m} \times 6 \mu\text{m}$ Nb patch that was protected

during the first RIE step. The chip then undergoes an identical SF_6 RIE step to remove the last of the Nb. The designed final dimensions of a typical HEB are 80 nm length \times 100 nm width \times 12 nm thickness (see FIG.3(g)).

Following device fabrication, an elliptical Si lens is affixed to the backside of the substrate. The lens is positioned within a well etched into the backside of the substrate. The well position is registered to within $\pm 5 \mu\text{m}$ of the device by means of an infrared backside contact aligner. This well is etched early in the process before device fabrication. The lens is affixed using purified bee's wax.

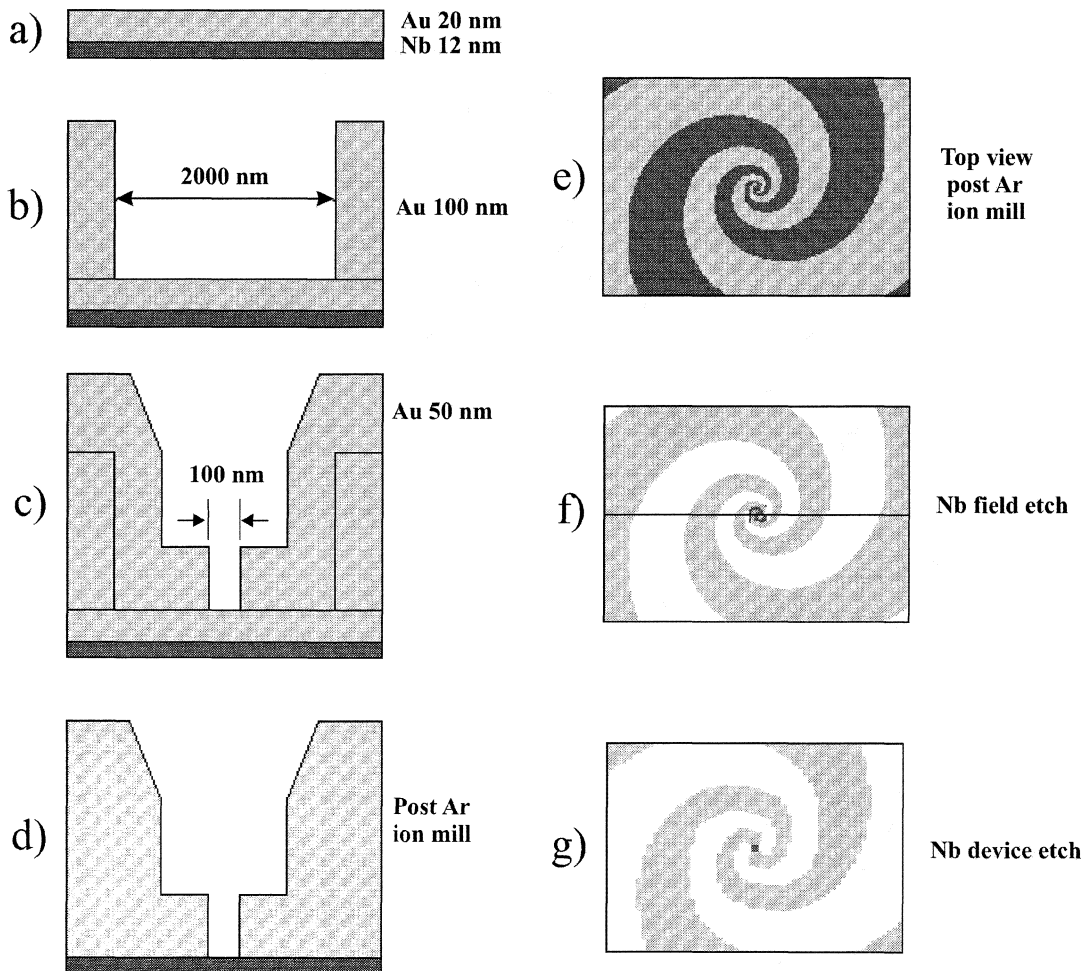


FIG.3. Device fabrication schematic.

III. OPTICAL LAYOUT

The apparatus for measuring noise temperatures is illustrated in FIG. 4. The mixer block is attached to an OFHC Cu pedestal on the cooled plate of a dewar. The base temperature is about 2 K, which is needed for Nb DHEB operation. The THz radiation enters the dewar through a quartz window and a reststrahl filter designed to block radiation above about 6 THz. The mixer is connected through a bias tee and a semi-rigid coaxial cable to a commercial cooled HEMT IF amplifier (L band) with a noise temperature of about 5 K.

The local oscillator signal is produced by an optically-pumped far-infrared laser. The laser is 1 m long and operates on most FIR laser lines between 30 and 300 μm . The polarization of the linearly polarized EH_{11} output mode can be rotated or converted to circular (if desired) by a polarization diplexer. The FIR laser and its CO_2 pump source run sealed off, but can be re-filled with gas of any isotopic composition. The output power of the free-running FIR laser is stable to better than 1 % over a period of several minutes, but is normally actively stabilized to better than 0.01 % long term by a closed-loop leveling circuit. FIG. 4 shows the GaAs Schottky diode sensor used for power control. An error signal generated from the difference between the diode's output and a reference voltage is used to control the CO_2 pump laser frequency, and hence the FIR laser's output power.

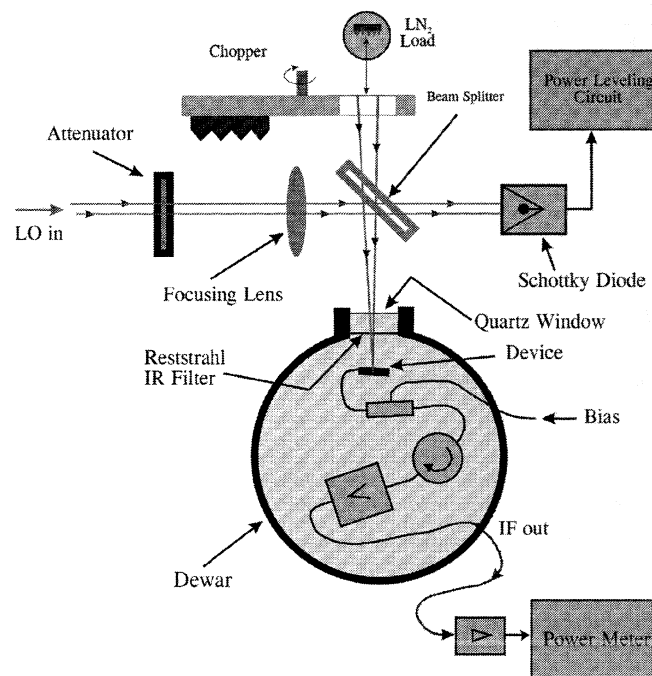


FIG. 4. Measurement setup for noise temperature.

IV. RESULTS AND DISCUSSION

Several DHEB devices were fabricated using the method described above. FIG.5(a) shows an SEM image of the device including the spiral antenna, whereas FIG. 5(b) shows an AFM image of the microbolometer at the antenna feeds. The gold banks of the antenna were aligned sufficiently well to accommodate the small microbolometer ($\sim 80 \text{ nm} \times 100 \text{ nm}$).

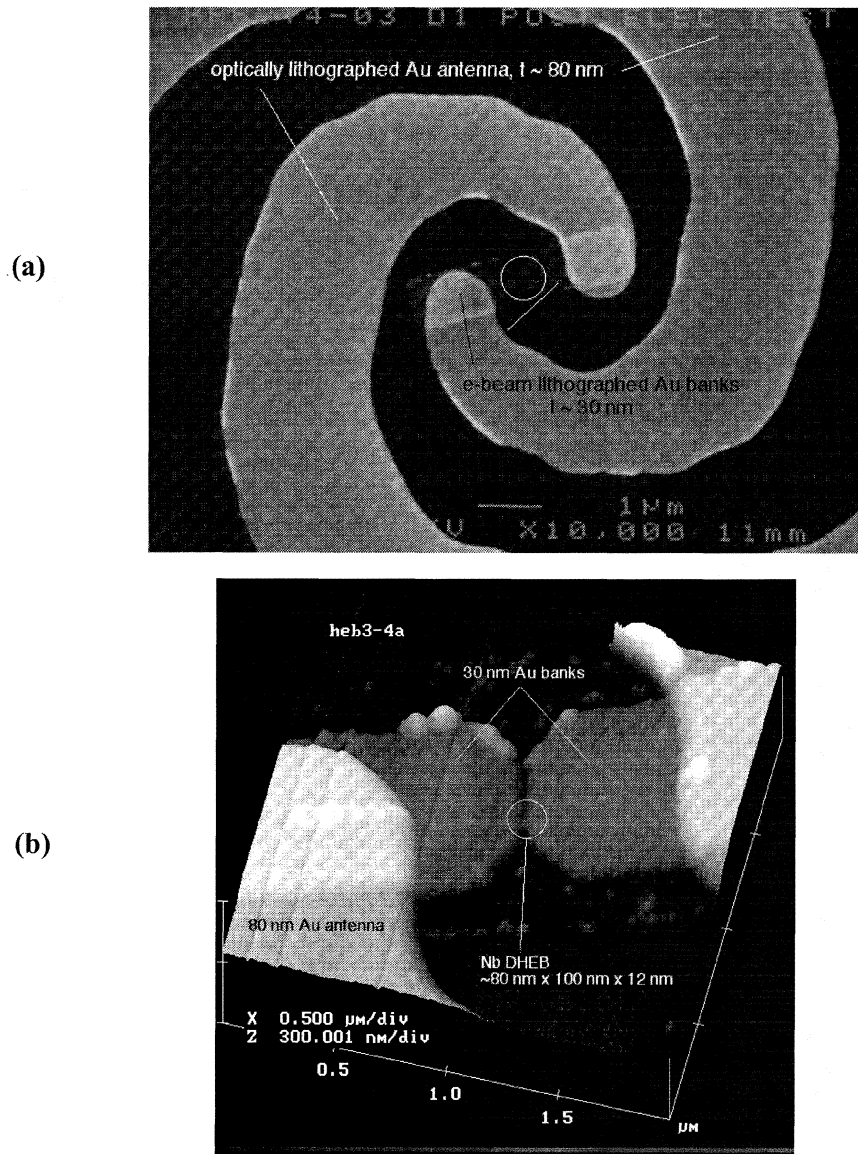


FIG.5. (a) SEM pictures of the DHEB, (b) AFM pictures of the DHEB.

The I-V characteristics of the device are shown in FIG. 6. The critical current is about 2.7 mA at a bath temperature of 2 K. The LO power centered at 2.52 THz (119 μm) was coupled to the device through a 6 μm beam splitter as illustrated in FIG. 4. The IF power was amplified by a cooled HEMT amplifier with 30 dB gain, a noise temperature of 5 K, and centered at 1 GHz. A room-temperature IF amplifier with a gain of 60 dB was used for additional amplification. Y-factor measurements between black body sources at room temperature and at N_2 (77K) were taken and Y-factors as high as 0.4 dB were observed. A reproducible double sideband receiver noise temperature of 2500 K was measured at the optimum bias point of 686 μV and 812 μA . This noise-temperature result was not corrected for losses and mismatches and therefore can be improved by better power coupling and IF matching circuitry. The power absorbed by the device was calculated from the constant resistance line (points (I) and (II) on FIG. 6), along which the hot electrons' temperature is constant, to be 4.9 μW . The total laser power of about 2.5 mW before the focusing lens and the beam splitter was not sufficient to pump the device optimally when a beam splitter with 8 % reflectivity was used. The total power coupling efficiency is estimated to be about 13 dB ($\sim 100 \mu\text{W}$ in front of the dewar). The device was therefore LO starved, which implies that a better DSB receiver noise temperature was possible with more LO power. The need for high LO power is consistent with the rela-

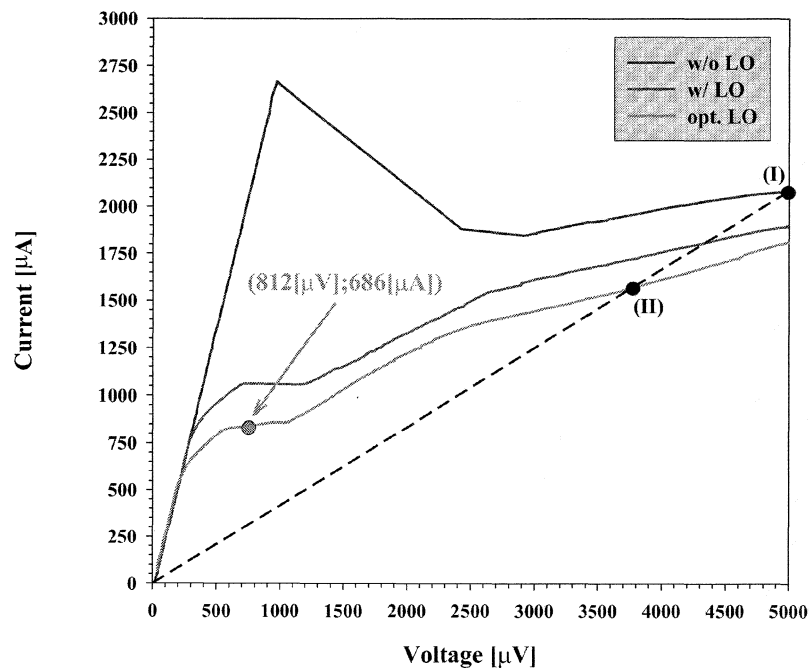


FIG. 6. I-V characteristics of the DHEB device.

tively high critical current. A microbolometer with a cross-sectional area of $100 \text{ nm} \times 12 \text{ nm}$ cannot support such a high critical current. We attribute the high critical current to the larger $6 \text{ }\mu\text{m} \times 6 \text{ }\mu\text{m}$ square area of Nb around the bridge that was not etched away entirely. Future efforts will correct this deficiency.

ACKNOWLEDGMENTS

This work was supported by the NASA Explorer/SOFIA Technology Development Program under Grant NAG5-8538.

REFERENCES

1. E. M. Gershenzon, G. N. Gol'tsman, I. G. Gogidze, Y. P. Gousev, A. I. Elant'ev, B. S. Karasik, and A.D. Semenov, "Millimeter and Submillimeter Range Mixer Based on Electronic Heating of Superconducting Films in the Resistive State", *Soviet Physics: Superconductivity*, 3, 1582, 1990
2. D.E. Prober, "Superconducting Terahertz Mixer Using a Transition-Edge Microbolometer," *Appl.Phys.Lett.*, 62, 2119, 1993.
3. R.Wyss, B.Karasik, W.R. McGrath, B. Bumble, and H. LeDuc, "Noise and Bandwidth Measurements of Diffusion-Cooled Nb HEB Mixers at Frequencies Above the Superconductive Energy Gap," *Proc. Tenth Intern. Space THz Technol. Symp.*, U.Virginia, March 1999, p. 214.
4. E. Gerecht, C.F. Musante, Y. Zhuang, M. Ji, K.S. Yngvesson, T. Goyette, and J. Waldman, "Development of Focal Plane Arrays Utilizing NbN Hot Electron Bolometric Mixers for the THz Regime," *Proc. Eleventh Intern. Space THz Technol. Symp.*, U. Michigan, May 2000.
5. A.L. Betz and R.T. Boreiko, "A Practical Schottky Mixer for 5 THz (Part II)," *Proc. Seventh Intern. Space THz Technol. Symp.*, , pp. 503-510, Charlottesville, VA, March 1996.
6. P. H. Siegel, "Terahertz Technology", *IEEE Trans. on Microw. Theo.and Techn.*, Vol. 50, No. 3, 910-928, March 2002.

7. S. Cherednichenko, M. Kroug, H. Merkel, P. Khosropanah, A. Adam, E. Kollberg, D. Loudkov, G. Gol'tsman, B. Voronov, H. Richter, and H.-W. Huebers, "1.6 THz Heterodyne Receiver for the Far Infrared Space Telescope", *Europ. Conf. on Applied Supercond.*, Copenhagen, August 2001.
8. A.D. Semenov, H.W. Huebers, J. Schubert, G. Gol'tsman, A.I. Elantiev, B. Voronov, and G. Gershenzon, "Design and performance of the lattice cooled hot-electron terahertz mixer", *J.Appl.Phys.* 88 (11), p.6758, 2000.
9. E. Gerecht, C. D. Reintsema, E. N. Grossman, A. L. Betz, and R. T. Boreiko, "Superconducting Nb DHEB Mixer Arrays for Far-Infrared Spectroscopy," *Proc. Twelfth Intern. Space THz Technol. Symp.*, JPL, February 2001.
10. E. N. Grossman, J. E. Sauvageau, and D. G. McDonald, "Lithographic Spiral Antennas at Short Wavelengths," *Appl. Phys. Lett.*, v. 59, p.3225, 1991.